

Density Functional Study on the Mechanism of Collision Reaction among Protons, N₂ and Water Vapor

SUN, Hao(孙昊) PAN, Xiu-Mei(潘秀梅) ZHAO, Min(赵岷)
LIU, Peng-Jun(刘朋军) SU, Zhong-Min(苏忠民) WANG, Rong-Shun*(王荣顺)

*Institute of Functional Material Chemistry, Faculty of Chemistry, Northeast Normal University,
Changchun, Jilin 130024, China*

The mechanism of collision reaction among protons, N₂ and water vapor was theoretically studied using Density Functional Theory. The geometries of reactants, transition states, intermediates and products were optimized at the B3LYP/6-311++G** level by the BERNY gradient analysis method. Transition states and intermediates have been identified by vibrational frequency analysis. The relationship among reactants, intermediates, transition states and products was affirmed by IRC calculation. The variations of energy and geometry along the IRC-determined reaction paths were described. The possible reaction pathways were represented and the optimal one was decided from the viewpoint of energy.

Keywords density functional theory, reaction mechanism, transition state, proton, N₂, water vapor

Introduction

Nitrogen gas, the main component of atmosphere, is always the hotspot in scientific studies, such as nitrogen fixation, to find feasible ways to dissociate its tri-bond and so on. In recent years, interstellar nitrides have attracted extensive attention in experimental and theoretical areas.^{1,2} In addition, there exist a great deal of water vapor and protons as well, the major components of cosmic rays, and therefore their reactions play a significant role in chemistry and biochemistry.³ There is also some indication that the reaction of those three by collision can generate hydrides and oxides of nitrogen and contribute to the destruction of ozone.⁴⁻⁶ The products, such as NNOH⁺ ions, can react with CH₄ and NO, and cause the atmospheric pollution.⁷ So a detailed study on the mechanism of this reaction is of great value and importance.

Computational methods

Full optimizations by means of Schlegel's algorithm⁸ at the B3LYP DFT level⁹ with the 6-311++G** basis set were performed using the Gaussian 98W program. The nature of the stationary points was further checked, and zero point vibrational energies (ZPVE) were evaluated by analytical computations of harmonic vibrational frequencies at the same theory level. Intrinsic reaction coordinate (IRC) calculations with the same method and level were also carried out to check the connection between all the critical structures located, using the Gon-

zalez and Schlegel method¹⁰ implemented in Gaussian 98W.

Results and discussion

Verification of intermediates and transition states

The results derived from our calculations confirm that there are five intermediates, eight transition states and two products on the potential energy surface (PES). The geometries and structural parameters of all stationary points are depicted in Figure 1.

In order to affirm the intermediates and transition states along the reaction pathways, we analyzed the vibrational frequencies of all the stationary points. All of them have twelve vibration fundamentals, but only TS1, TS2, TS3, TS4, TS5, TS6, TS7 and TS8 have merely one vibration fundamental which has an imaginary frequency, and consequently are proved to be really transition states. Their imaginary frequencies are 1854.4312i cm⁻¹ (TS1), 816.6063i cm⁻¹ (TS2), 1601.1969i cm⁻¹ (TS3), 1292.9153i cm⁻¹ (TS4), 718.7362i cm⁻¹ (TS5), 392.6493i cm⁻¹ (TS6), 98.4653i cm⁻¹ (TS7), 356.3885i cm⁻¹ (TS8), respectively. The cartesian displacement vectors associated with the imaginary vibration frequencies of the transition states are listed in Table 1. While the vibrational frequencies of IM1, IM2, IM3, IM4 and IM5 are all real and positive, which implies that they are all minima on the PES. The connections of reactants, intermediates, transition states and products

* E-mail: wangrs@nenu.edu.cn; Fax: 86-431-5684009

Received October 23, 2003, revised and accepted February 8, 2004.

Project supported by Ministry of Education (the training project of elitist) Foundation (No. [2001]3) and the Young Teacher Fund of Northeast Normal University (No. 111382).

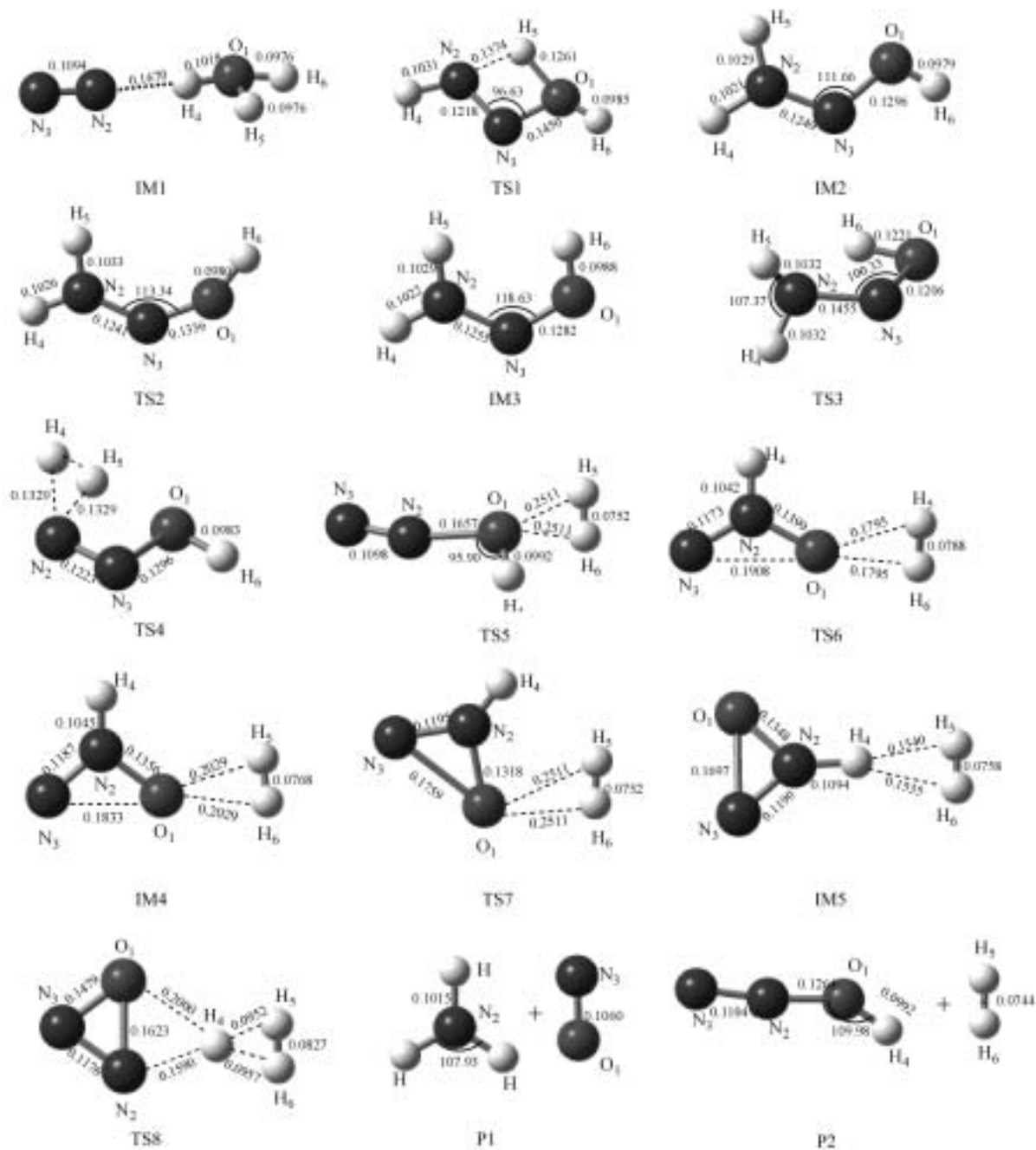


Figure 1 Geometries of all the species at the pathways (unit: bond length in nm, bond angle in degree).

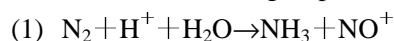
are further affirmed by IRC calculation, indicating that they are located on the correct pathways.

Analysis of reaction mechanism

It was reported that the rate constant for the reaction $\text{N}_2\text{H}^+ + \text{H}_2\text{O} \rightarrow \text{H}_3\text{O}^+ + \text{N}_2$ is $(2.5 \pm 0.7) \times 10^{-9} \text{ cm}^3 \cdot \text{sec}^{-1}$ at 300 K,¹¹ and our study has also shown that the system of the above products is much more stable. So we begin the reaction of N_2 , water vapor and a proton with H_3O^+ and N_2 (IM1). Heat (726.26 kJ/mol) released in this step is sufficient for the next steps. The energies of all species are listed in Table 2 and potential energy surface is depicted in Figure 2.

According to our computational results, the title

reaction is a dual-channel process. The reaction can be represented as the following steps:



The products NH_3 and NO^+ from channel (1) can be generated via the route $\text{R} \rightarrow \text{IM1} \rightarrow \text{TS1} \rightarrow \text{IM2} \rightarrow \text{TS2} \rightarrow \text{IM3} \rightarrow \text{TS3} \rightarrow \text{P1}$. Hydrogen transference ($\text{TS1} \rightarrow \text{IM2}$) and single bond rotation ($\text{IM2} \rightarrow \text{TS2} \rightarrow \text{IM3}$) go through successively, and whereafter another hydrogen transference and concomitant chemical bond break ($\text{IM3} \rightarrow \text{TS3} \rightarrow \text{P1}$) result in the product 1 (NH_3 and NO^+). The barrier height for such process is 438.29 kJ/mol and

Table 1 Vibration models of imaginary frequencies of all transition states

| Transition states | TS1 | | | TS2 | | | TS3 | | | TS4 | | |
|--|------------|-------|-------|-----------|-------|-------|------------|-------|-------|------------|-------|-------|
| Imaginary frequencies/cm ⁻¹ | 1854.4312i | | | 816.6063i | | | 1601.1969i | | | 1292.9153i | | |
| Coordinates | X | Y | Z | X | Y | Z | X | Y | Z | X | Y | Z |
| O(1) | 0.00 | 0.03 | 0.00 | -0.04 | 0.08 | -0.04 | -0.01 | 0.03 | 0.00 | -0.01 | 0.01 | 0.00 |
| N(2) | 0.03 | -0.02 | 0.00 | 0.01 | -0.01 | -0.04 | -0.02 | -0.03 | 0.00 | -0.04 | 0.13 | 0.00 |
| N(3) | 0.04 | 0.00 | 0.00 | -0.01 | -0.00 | 0.07 | -0.04 | 0.01 | 0.00 | 0.06 | -0.05 | 0.00 |
| H(4) | 0.00 | -0.12 | -0.02 | 0.00 | 0.01 | -0.03 | -0.01 | -0.11 | -0.02 | -0.03 | -0.66 | 0.23 |
| H(5) | -0.97 | -0.14 | -0.01 | 0.07 | -0.02 | -0.12 | -0.01 | -0.11 | 0.02 | -0.03 | -0.66 | -0.23 |
| H(6) | 0.00 | 0.13 | -0.06 | 0.47 | -0.82 | 0.27 | 0.99 | 0.00 | 0.00 | 0.00 | 0.02 | 0.00 |
| Transition states | TS5 | | | TS6 | | | TS7 | | | TS8 | | |
| Imaginary frequencies/cm ⁻¹ | 718.7362i | | | 392.6493i | | | 98.4653i | | | 356.3885i | | |
| Coordinates | X | Y | Z | X | Y | Z | X | Y | Z | X | Y | Z |
| O(1) | 0.31 | -0.04 | 0.00 | 0.24 | -0.02 | 0.00 | -0.09 | 0.11 | 0.00 | 0.10 | 0.02 | 0.00 |
| N(2) | -0.16 | 0.07 | 0.00 | -0.12 | 0.01 | 0.00 | 0.07 | 0.03 | 0.00 | -0.10 | 0.11 | 0.00 |
| N(3) | -0.11 | -0.04 | 0.00 | -0.06 | -0.03 | 0.00 | 0.02 | -0.07 | 0.00 | -0.03 | -0.03 | 0.00 |
| H(4) | 0.05 | 0.01 | 0.00 | -0.05 | 0.02 | 0.00 | 0.20 | 0.09 | 0.00 | 0.06 | -0.77 | 0.00 |
| H(5) | -0.63 | 0.14 | 0.09 | -0.61 | 0.30 | -0.05 | -0.05 | -0.68 | 0.00 | 0.20 | -0.45 | 0.00 |
| H(6) | -0.63 | 0.14 | -0.09 | -0.61 | 0.30 | 0.05 | -0.05 | -0.68 | 0.00 | -0.10 | -0.34 | 0.00 |

Table 2 Energies of all stationary points on the potential energy surface of reaction

| System | E^a /a.u. | $Z-PC^b$ /a.u. | E_0^c /a.u. | E_R^d /a.u. | E_R^d /($\text{kJ}\cdot\text{mol}^{-1}$) |
|--------|-------------|----------------|---------------|---------------|--|
| R | -186.01815 | 0.02685 | -185.99130 | 0.00000 | 0 |
| IM1 | -186.30907 | 0.04220 | -186.26687 | -0.27557 | -726.2762 |
| TS1 | -186.14033 | 0.03976 | -186.10057 | -0.10927 | -287.9857 |
| IM2 | -186.22256 | 0.04706 | -186.17550 | -0.18420 | -485.4667 |
| TS2 | -186.18602 | 0.04445 | -186.14157 | -0.15027 | -396.0429 |
| IM3 | -186.20328 | 0.04632 | -186.15696 | -0.16566 | -436.6039 |
| TS3 | -186.12125 | 0.04007 | -186.08118 | -0.08988 | -236.8825 |
| TS4 | -186.07018 | 0.03434 | -186.03584 | -0.04454 | -117.3871 |
| TS5 | -186.08851 | 0.03233 | -186.05618 | -0.06488 | -170.9940 |
| TS6 | -185.99006 | 0.03087 | -185.95919 | 0.03211 | 84.6278 |
| IM4 | -185.99044 | 0.03139 | -185.95905 | 0.03225 | 84.9962 |
| TS7 | -185.98902 | 0.03127 | -185.95775 | 0.03355 | 88.4224 |
| IM5 | -185.99638 | 0.03181 | -185.96457 | 0.02673 | 70.4480 |
| TS8 | -185.97169 | 0.02932 | -185.94237 | 0.04893 | 128.9570 |
| P1 | -186.22538 | 0.04375 | -186.18163 | -0.19033 | -501.6228 |
| P2 | -186.13043 | 0.03467 | -186.09576 | -0.10446 | -275.3087 |

^a Uncorrected energies; ^b zero-point correction; ^c sum of electronic and zero-point energies; ^d relative energies to reactants.

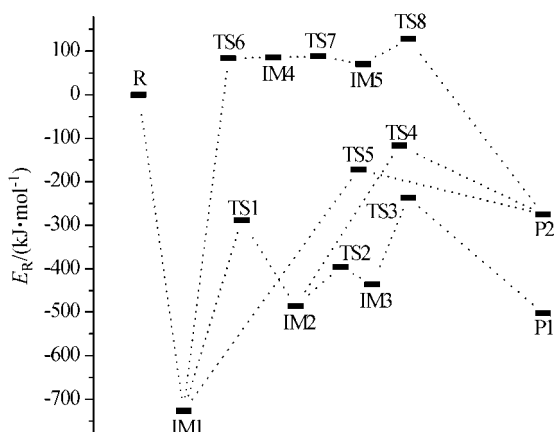


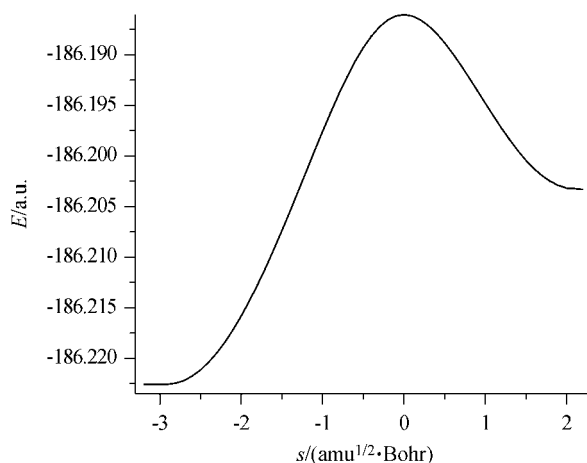
Figure 2 Variation of energy along the pathways.

the heat of 501.62 kJ/mol is set out to produce P1. The isomerization between IM2 and IM3 will be discussed in the following text.

P2 ($\text{NNOH}^+ + \text{H}_2$) can be obtained along three routes.



As for route 2.1, similar to channel (1), the process of $\text{R} \rightarrow \text{IM1} \rightarrow \text{TS1} \rightarrow \text{IM2}$ comes through at the first and equal barrier height is overcome, and then two H atoms connected with N(2) are gradually dissociated and P2 is generated via TS4 with a heat energy of 275.31 kJ/mol released. P2 can also be achieved through route 2.2, via IM1 and TS5. The energy of TS5 is 555.28 kJ/mol higher than IM1. The third possible route to generate P2 is $\text{R} \rightarrow \text{IM1} \rightarrow \text{TS6} \rightarrow \text{IM4} \rightarrow \text{TS7} \rightarrow \text{IM5} \rightarrow \text{TS8} \rightarrow \text{P2}$. TS6 has the energy of 641.75 kJ/mol higher than IM1, and the activation energy is 203.46 kJ/mol higher than route (1) and 2.1, 86.47 kJ/mol higher than route 2.2.



Isomerization of intermediates

The step $\text{IM2} \rightarrow \text{TS2} \rightarrow \text{IM3}$ involves a typical isomerisation of the two intermediates. The isomerization steps are important in determining the overall rate and yield,^{12,13} so we will discuss the isomerization process in detail. There is an energy barrier of 89.43 kJ/mol for N—O bond rotation step $\text{IM2} \rightarrow \text{TS2}$ whereas the barrier for $\text{IM3} \rightarrow \text{TS2}$ is 40.56 kJ/mol. The variation of energy and important geometry parameters are shown in Figure 3. From the figure, we can see that only $\angle 6132$ changes much during N—O bond rotation, and IM2 is much more stable than IM3 because of its faint spatial repulsion.

Energy changes on the pathways

To obtain the variation of energy along the path of the reaction, IRC calculations at the level of B3LYP/6-311 + G** were carried out. Calculations were started from all transition states by a step-length of 0.1 amu^(1/2)·Bohr, following the least energy path forward and backward scanning 100 points. Taking the reactant energy as zero, we calculated relative energy for each stationary point. Energy change along the reaction path is shown in Figure 3, which describes the mechanism of the collision reaction among protons, N₂ and water vapor.

Conclusion

The title reaction is a multi-channel and exothermic process. The reaction can be represented as the steps below:

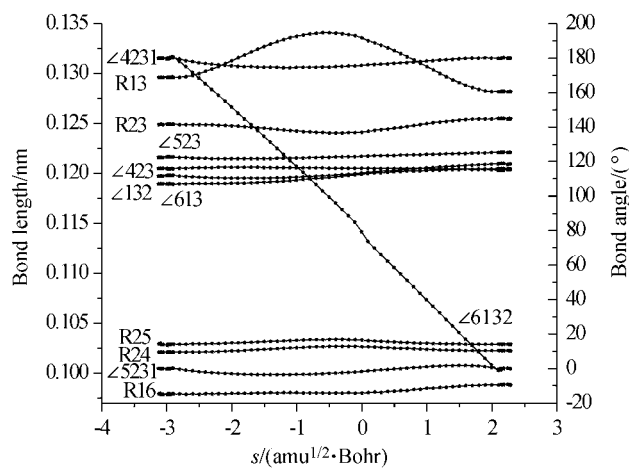


Figure 3 Variation of energy during isomerization process $\text{IM2} \rightarrow \text{TS2} \rightarrow \text{IM3}$ and variation of important geometry parameters.

IM1→TS1 is the rate-determining step of route (1). The energy barrier height of this route is the lowest and P1 is more stable than P2, and therefore route (1) is the optimal route for this reaction. Considering its higher energy and insurmountable activation energies, P2 is not considered as the optimistic product, although P2 can be achieved via three routes and its branch ratio is larger than that for P1.

Our investigation in the present paper may be prospective to contribute to the study on interstellar molecular reactions.

References

- 1 Chi, Y.-J.; Yu, H.-T.; Fu, H.-G.; Xin, B. F.; Li, Z.-S.; Sun, J.-Z. *Chin. J. Chem.* **2003**, *21*, 30.
- 2 Liu, P.-J.; Pan, X.-M.; Zhao, M.; Sun, H.; Su, Z.-M.; Wang, R.-S. *Acta Chim. Sinica* **2002**, *11*, 1941 (in Chinese).
- 3 Kobayashi, K.; Kaneko, T.; Saito, T. *Adv. Space. Res.* **1999**, *24*, 461.
- 4 Li, L.-C.; Wang, X.; Tian, A.-M. *Acta Chim. Sinica* **2000**, *58*, 1099 (in Chinese).
- 5 Nguyen, M. T.; Hegarty, A. F. *J. Chem. Soc., Perkin Trans. 2* **1987**, *2*, 345.
- 6 Bagno, A.; Scorrano, G. *J. Phys. Chem.* **1996**, *100*, 1536.
- 7 Ferguson, E. E. *Chem. Phys. Lett.* **1989**, *156*, 319.
- 8 Schlegel, H. B. *J. Comput. Chem.* **1982**, *3*, 214.
- 9 (a) Becke, A. B. *J. Chem. Phys.* **1993**, *98*, 5648.
(b) Becke, A. B. *Phys. Rev. A* **1998**, *38*, 3098.
(c) Lee, C.; Yang, W.; Parr, R. G. *Phys. Rev. B* **1998**, *37*, 785.
- 10 (a) Gonzalez, C.; Schlegel, H. B. *J. Chem. Phys.* **1989**, *90*, 2154.
(b) Gonzalez, C.; Schlegel, H. B. *J. Phys. Chem.* **1990**, *94*, 5523.
- 11 Bolden, R. C.; Jeffs, S. P.; Twiddy, N. D. *Chem. Phys. Lett.* **1973**, *23*, 73.
- 12 Pan, X.-M.; Wang, R.-S.; Su, Z.-M.; Tyrrell, J. *Chem. J. Chin. Univ.* **2001**, *22*, 2077 (in Chinese).
- 13 Pan, X.-M.; Su, Z.-M.; Wang, R.-S. *J. Chem. Phys.* **1995**, *8*, 314.

(E0310233 ZHAO, X. J.)